

Quantum-Chemical Study on the Effect of Lewis Acid Centers in a Poly(ethylene oxide)-Based Solid Electrolyte

Andrzej Eilmes* and Piotr Kubisiak

Faculty of Chemistry, Jagiellonian University, Ingardena 3, 30-060 Kraków, Poland

Received: February 28, 2007; In Final Form: May 14, 2007

Quantum-chemical calculations on borate and aluminate esters have been performed to study the effect of a Lewis acid center on the ion complexation in a poly(ethylene oxide)-based solid electrolyte. The preferred conformations of the investigated model molecules have been determined. Stabilization energies for Li^+ and ClO_4^- ions complexed at the boron or aluminum center have been calculated. The results reveal that the stabilization of the perchlorate ion at the boron center is mainly due to the interactions with CH_2 and CH_3 groups and suggest much stronger binding of the anion to the aluminum atom.

I. Introduction

Polymer-based solid electrolytes continue to attract significant attention due to their application in lithium batteries, solid-state electrochemical devices, sensors, displays, electrochromic devices, etc. An electrolyte of such a type consists of an inorganic salt dissolved in a polymer matrix, e.g., a lithium salt in poly(ethylene oxide) (PEO). A considerable effort has been made to improve the performance of electrolytes for a particular application.

One of the routes to increase cation transport numbers and the overall conductivity of the electrolyte is to modify cation–anion and anion–polymer interactions. This can be achieved by adding Lewis acid centers into the electrolyte. There are numerous recent experimental works introducing boron^{1–7} or aluminum^{3,8–10} atoms as Lewis acids. The acid center may be incorporated directly into the polymer structure^{1,2,5,7,9} or added in a plasticizer molecule.^{4,6,10}

An increase of the cation transport number in such an electrolyte is explained as the effect of anion trapping by acidic centers which facilitates dissociation of anion–cation pairs and increases the number of free cations. It would be interesting to examine theoretically how efficient such anion binding may be in different electrolytes.

This paper is devoted to a quantum-chemical study of ion interactions with a boron or aluminum center. Because of their large computational cost *ab initio* calculations are limited to relatively small systems. In the research on PEO-based solid electrolytes they were used to study small molecules modeling the polymer backbone (e.g., dimethoxyethane,^{11,12} diglyme,¹³ or ethylene glycol oligomers¹⁴), cation–anion pairs,¹⁵ or ion interactions with the polymer.^{16–22} Based on such calculations several force-field parametrizations have been developed.^{23–28}

Following this route we will study the effect of Lewis acid centers on the complexation of Li^+ and ClO_4^- ions in the PEO-based electrolyte. The energetic effect of the boron atom on the interaction with the perchlorate anion has been recently calculated in ref 6 from the electronegativities and hardnesses of the complex constituents based on the hard and soft acids and bases theory. In this paper we use quantum-chemical

calculations (mainly density functional theory, DFT) to investigate in more detail the interactions of the ions with esters containing boron or aluminum atoms as Lewis acids. First, in section II, we perform a search for low-energy conformations of some molecules modeling the acid center in polymers. These structures then become the starting point for the study of ion complexation and for the comparison of stabilization energies for complexes with borate and aluminate compounds; the results of this analysis are presented in section III. We summarize and conclude in section IV.

II. Conformational Studies

Methodology. Our set of model molecules consists of trimethoxyborane $\text{B}(\text{OCH}_3)_3$ (TMB) and tri(methoxyethoxy)borane $\text{B}(\text{OCH}_2\text{CH}_2\text{OCH}_3)_3$ (TMEB) and their aluminum equivalents trimethoxyaluminum $\text{Al}(\text{OCH}_3)_3$ (TMAI) or tri(methoxyethoxy)aluminum $\text{Al}(\text{OCH}_2\text{CH}_2\text{OCH}_3)_3$ (TMEAI). The boron or aluminum atom represents the acid center in branched PEO, and the alkoxy groups correspond to the $\text{CH}_2\text{CH}_2\text{O}$ repeat units of the polymer backbone. The smaller molecules are used to gain some physical insight at low computational cost, while the larger (and more computationally demanding) molecules allow more flexibility of the side chains and therefore are supposed to better mimic the real polymer system. Compounds like TMEB or TMAI (with longer alkoxy chains) have been also used as plasticizers carrying the acid center.^{4,6,10}

All calculations reported in this paper were performed using the Gaussian03 program.²⁹ Our search for low-energy conformers of the investigated molecules began with a preliminary geometry optimization at the semiempirical level of theory. The set of initial structures for the TMB molecule (about 21 000 structures) was generated in a systematic way by changing the torsional angles for B–O and C–O bonds in steps of 30°. Geometry optimization using the MNDO method allowed us to select a limited number of structures, which were then further optimized in DFT calculations with the B3LYP functional. In the case of the TMAI molecule initial geometries for DFT optimization were created from the results of MNDO optimization for TMB by substituting boron with aluminum atoms.

The systematic creation of initial geometries for TMEB and TMEAI in the above-described way would lead to a huge number of structures and to a prohibitively large computational

* Corresponding author fax: +48126340515; e-mail: eilmes@chemia.uj.edu.pl.

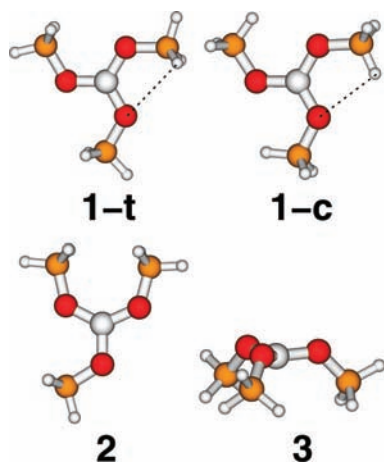


Figure 1. Geometries of the trimethoxyborane molecule conformers optimized at the B3LYP/aug-cc-pVDZ level (except for structure 3 obtained from the semiempirical MNDO calculations).

TABLE 1: Energies (kcal/mol) of TMB Conformers from the B3LYP Calculations^a

conformer	3-21G	6-31G**	aug-cc-pVDZ	aug-cc-pVTZ
1- <i>t</i>	1.25	0.00	0.00	0.00
1- <i>c</i>	0.00	0.13	0.91	0.72
2	8.95	7.64	7.50	7.50
3 ^a	35.89	33.23	34.09	33.85

^a Geometries of conformers 1 and 2 were optimized in the B3LYP calculations. Energies for conformer 3 were obtained from single-point DFT calculations for MNDO geometry.

effort during optimization. Therefore the sets of initial structures (about 1000 per molecule) were obtained by random choice of torsional angles. Subsequent semiempirical and DFT geometry optimizations were then performed in a similar way as for the TMB and TMAI molecules. As an additional check we performed single-point Møller–Plesset (MP2) calculations for selected geometries obtained in DFT calculations.

Except for the TMB molecule we did not perform further checks whether the stationary point found in the quantum-chemical calculations corresponds to the minimum or a saddle point on the energy surface as this is not an important issue for the calculations of complexation energies. On the other hand, gathering information on stationary points, irrespective of their type, will be useful for future force-field development for such compounds.

Trimethoxyborane and Trimethoxyaluminum. In Figure 1 we display four conformers of the TMB molecule, and their energies calculated at different levels of theory are listed in Table 1. All non-hydrogen atoms in the 1-*c*, 1-*t*, and 2 structures are coplanar. The 1-*c* and 1-*t* structures exhibit C_{3h} symmetry and differ in the orientation of methyl groups—the in-plane hydrogen atoms of the CH_3 groups are located either in a cis or trans position with respect to the boron atom. The geometries of conformers 1 and 2 optimized in DFT B3LYP do not depend significantly on the basis set (6-31G** or Dunning’s aug-cc-pVDZ) used in the calculations. The “umbrella”-shaped conformer 3 of much higher energy corresponds to a stationary point only in semiempirical calculations and during optimization at the DFT level changes to structure 2, slightly distorted from planar geometry.

We will discuss structures 1-*c* and 1-*t* in more detail as there are relevant experimental data available. According to the data listed in Table 1, in the calculations using the small basis set 3-21G the lowest-energy conformer is the 1-*c* structure in agreement with the Hartree–Fock (HF) calculations of ref 30.

TABLE 2: Experimental and Calculated Harmonic Frequencies for the 1-Trans Conformer of TMB

symmetry	exp ^a	exp ^b	calc ^c	
A'	317	310	300	
	729	732	730	
	1125	1120	1123	
	1183	1208	1224	
	1450	1445	1454	
	1470	1461	1473	
	2867	2876	3032	
	2942	2978	3130	
	A''			81
		102	103	110
667		669	682	
1115		1184	1164	
1489		1509	1471	
2964		2980	3101	
E'		187	189	175
	521	521	520	
	1041	1040	1042	
	1204	1179	1184	
	1364	1362	1360	
	1468	1487	1468	
	1510	1494	1492	
	2882	2884	3031	
	2953	3000	3130	
	E''	165	78	72
230		131	183	
1165		1162	1164	
1485		1470	1470	
2974		2996	3100	

^a Reference 33. ^b Reference 31. ^c Results of this work B3LYP/aug-cc-pVDZ calculations.

For larger basis sets the relative energy of the 1-*c* structure increases compared to that of 1-*t*, and the trans conformer becomes the most stable one, as seen in HF/4-31G and HF/6-31G* calculations.³¹ We have found this dependence also in HF and MP2 calculations for basis sets up to aug-cc-pVDZ.

We have calculated geometrical parameters of the lowest-energy conformer of TMB in different basis sets (3-21G, 6-31G** and aug-cc-pVDZ) and compared them to the experimental data obtained in ref 32 from electron diffraction measurements in the gas phase (the full set of data is presented in the Supporting Information). The calculated bond lengths and angles compare reasonably well to the experiment, apart from the value of the dihedral angle HCOB and the distance between O_1 and H_4 (indicated by a dashed line in Figure 1). For basis sets larger than 3-21G the HCOB angle is about 60° , which corresponds to the trans geometry. The experimental data fit the cis structure better, although the value 23.6° of the torsional angle reported in ref 32 deviates significantly from 0° . It should be noted that the calculated (B3LYP/aug-cc-pVDZ) energy barrier for the rotation of a single CH_3 group in TMB (with the rest of the molecule frozen) is about 0.6 kcal/mol; therefore, one should expect that both conformations are populated. In view of the above results it is not certain which of them is the most stable one.

In Table 2 we present the harmonic frequencies calculated for the 1-*t* conformer at the B3LYP/aug-cc-pVDZ level of theory and compare them to the experimental assignments from refs 33 and 31. The calculated values are in slightly better agreement with the more recent experimental data;³¹ an improvement compared to previous HF/3-21G calculations^{30,31} is noticeable (RMS error reduced by a factor of 2.8). Vibrational analysis for the cis configuration yields two imaginary frequencies of the torsional movements of CH_3 groups, which is an additional indication that the 1-*c* structure does not correspond to the energy minimum.

TABLE 3: Structural Parameters of TMB and TMAI Molecules Calculated at the B3LYP/aug-cc-pVDZ Level

TMB			
conformer no.	B–O (Å)	O–C (Å)	O–B–O (deg)
1- <i>c</i> , 1- <i>t</i>	1.371	1.427–1.429	120
2, 2a ^a	1.369–1.379	1.420–1.426	114–129
TMAI			
conformer no.	Al–O (Å)	O–C (Å)	O–Al–O (deg)
1- <i>c</i> , 1- <i>t</i>	1.712–1.713	1.417	120
2, 2 ^a	1.709–1.718	1.412–1.416	117–125

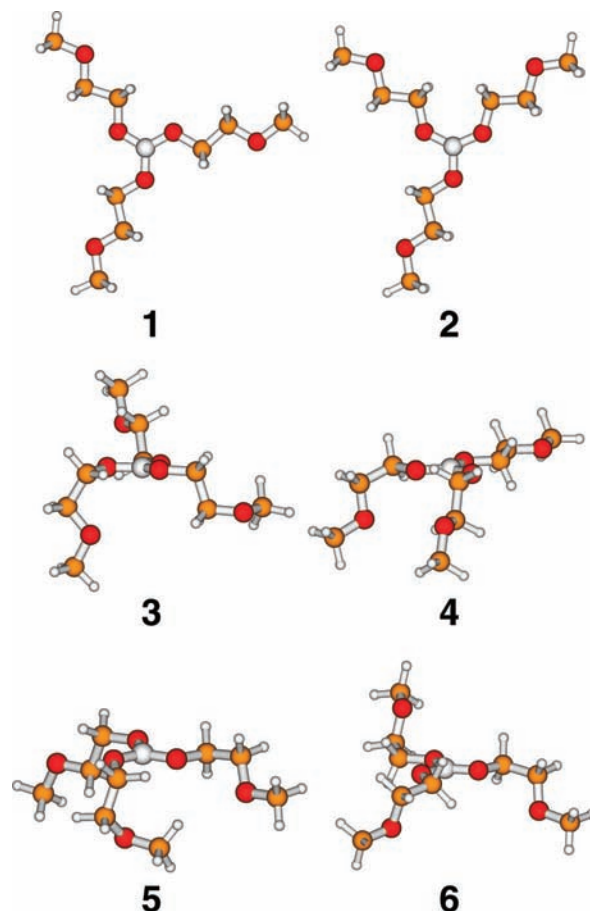
^a Structure 2a is a slightly distorted conformer 2 (not shown in Figure 1).

The geometries obtained for the TMAI molecule are similar to those shown in Figure 1, hence we do not display them separately. The *cis* conformer has the lowest energy; it should be noted, though, that the energy differences between TMAI conformers are smaller compared to those obtained for its boron analogue. This applies also to the nonplanar structure 4 which during B3LYP/aug-cc-pVDZ calculations converges to the distorted structure 2 as it was observed for the corresponding conformer of TMB.

The structural parameters for TMB and TMAI molecules obtained in the B3LYP/aug-cc-pVDZ calculations are collected in Table 3. The major difference is the large Al–O bond length; a secondary effect is the small shortening of the O–C bonds in the aluminate molecule.

Tri(methoxyethoxy)borane and Tri(methoxyethoxy)aluminum. The TMEB and TMEAI molecules contain the PEO repeat units CH₂CH₂O and therefore are more suitable to model the structure of the polymer and its interactions with ions. Flexibility of the methoxyethoxy groups leads to a large number of possible conformers. We performed the search for low-energy conformers in the way described at the beginning of section II. The DFT optimization step was applied to a set of geometries found in the semiempirical calculations, supplemented by some planar structures chosen in order to facilitate the comparison with the TMB and TMAI molecules.

Figure 2 shows the geometries of TMEB optimized at the B3LYP/aug-cc-pVDZ level; their relative energies are listed in Table 4. The energy difference between planar geometries 1 and 2 is about 6.5 kcal/mol, very close to that calculated for structures 1 and 2 of TMB. The *trans* conformer of structure 1 corresponds to the energy minimum. Based on B3LYP/6-311+G**//HF/3-21G calculations the 1-*trans* geometry has been predicted in ref 6 as the most stable conformer. According to our results it is indeed one of the low-energy conformers but not necessarily the lowest one. There are some nonplanar structures with energies comparable to that of structure 1 or even about 1–2 kcal/mol lower. However, further calculations show that the energies of such structures relative to the energy of 1-*t* geometry increase with increasing size of the basis set, as seen from the third column of Table 4. The DFT calculations suggest structure 1 to be the most stable conformer with accuracy of about 1 kcal/mol. We performed additional MP2/aug-cc-pVDZ single-point energy calculations for geometries obtained at the B3LYP/aug-cc-pVDZ level. We observed the increasing stabilization of nonplanar conformers relative to structure 1; the largest effect appears for structure 5, which is about 3.4 kcal/mol more stable than planar conformer 1. The difference in the relative MP2 energies compared to the B3LYP results may be attributed to the dispersion interactions which are underestimated in the DFT calculations. We can conclude

**Figure 2.** Low-energy conformers of the tri(methoxyethoxy)borane molecule calculated at the B3LYP/aug-cc-pVDZ level.**TABLE 4: Energies (kcal/mol) of the TMEB and TMEAI Conformers from the B3LYP Calculations**

conformer ^a	TMEB		TMEAI	
	6-31G** ^b	aug-cc-pVDZ	6-31G** ^b	aug-cc-pVDZ
1	0.00	0.00	0.00	0.00
2	6.58	6.55	1.38	1.07
3	0.17	1.34	−19.51	−15.41
4	−0.79	−0.12	−21.96	−16.87
5	−1.67	0.09	−30.71	−24.02
6	−0.67	−0.28	−33.37	−26.58

^a Conformers of TMEB and TMEAI numbered according to Figures 2 and 3, respectively. ^b Geometries of structures optimized at the 6-31G** level are close to those shown in Figures 2 and 3.

that there is a possibility that some nonplanar conformers are slightly more stable than structure 1.

The situation is different in the case of the TMEAI molecule (Figure 3 and Table 4). The energy differences between planar geometries 1 and 2 are comparable to those obtained for TMAI. The planar structures are without any doubts not the lowest-energy conformers. There are many nonplanar structures (a few examples are shown in Figure 3) which have significantly lower energy (the difference being up to 20–30 kcal/mol in DFT calculations and increasing up to 40 kcal/mol in single-point MP2 calculations). In these structures one or two oxygen atoms from the methoxyethoxy group approach closely (down to 1.98 Å) the aluminum atom. This may be rationalized as a result of electrostatic interactions. The fit of partial charges to the electrostatic potential around the molecule (using Merz–Kollman method,³⁴ as implemented in Gaussian03) shows that the partial positive charge located on the Al atom is about +0.4e

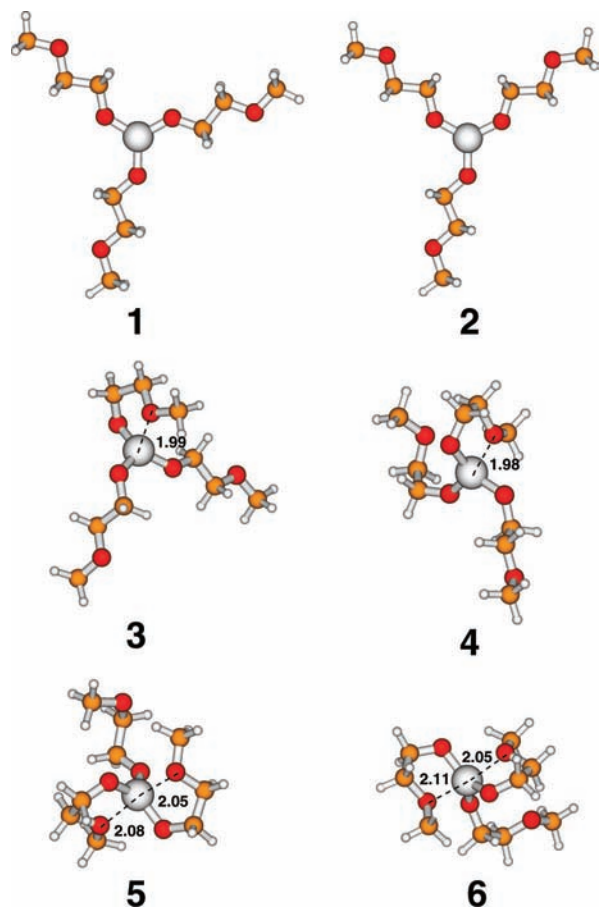


Figure 3. Low-energy conformers of the tri(methoxyethoxy)aluminum molecule calculated at the B3LYP/aug-cc-pVDZ level. Some interatomic distances (in Å) have been marked by dashed lines.

TABLE 5: Structural Parameters of TMEB and TMEAl Molecules Calculated at the B3LYP/aug-cc-pVDZ Level

TMEB				
conformer no.	B–O (Å)	O–C ^a (Å)	O–B–O (deg)	O–O–O–B (deg)
1	1.371	1.432	120	0
2	1.372–1.376	1.424–1.427	114–129	0
3–6	1.370–1.374	1.429–1.432	119–120	0–1
TMEAl				
conformer no.	Al–O (Å)	O–C ^a (Å)	O–Al–O (deg)	O–O–O–Al (deg)
1	1.712	1.419–1.420	120	0
2	1.709–1.717	1.417–1.419	116–124	0
3, 4	1.731–1.772	1.404–1.412	113–121	16–19
5, 6	1.760–1.788	1.396–1.405	115–128	0–1

^a Length of O–C bonds closest to the B or Al atom.

larger than the charge on the boron atom (e.g., about $+1.6e \div 1.7e$ for Al compared to $+1.2e \div +1.3e$ for B in structures 1 and 2). Electrostatic stabilization due to the interaction with negatively charged oxygen atoms is therefore large enough to favor the bending of the alkoxy chains. This conclusion is corroborated by the fact that the structures with two short Al–O contacts (e.g., complex 5 or 6) have lower energies than the conformers with one such contact (e.g., structure 3 or 4).

Table 5 collects the structural parameters for different conformers of TMEB and TMEAl. It is noticeable that in the structures with one Al–O contact the four central atoms are not coplanar—the Al atom is shifted toward oxygen. The length of the Al–O bond in bent structures is larger than in planar

conformers, while the neighboring O–C bonds are shorter; both lengths vary in quite a broad range.

Based on these calculations one may expect that the type of the Lewis acid center (Al or B) will affect the local structure of polymer chains in its neighborhood. The aluminum atom is likely to introduce extra bends into the polymer structure, while the bent conformations at the boron center are not so strongly favored, since the energy differences between the planar and nonplanar structures are much smaller.

III. Ion Complexation

The conformers found in the preceding section were subsequently used in a study of ion complexation. It is expected that lithium cations will interact with the base sites (oxygen atoms from the alkoxy groups), whereas the anions will be trapped by Lewis acids (boron or aluminum atoms). The magnitude of such effects and the possible complex structures may be predicted based on the values of the electrostatic potential around our model molecules (Figure 4).

In the molecular plane of the conformers 1 and 2 of TMB and TMAI the regions of negative electrostatic potential are concentrated near the oxygen atoms, while positive potential values are located close to the methyl groups. Within the plane the preferable position for perchlorate ions will be therefore close to the terminal CH₃ groups. The lithium cations will tend to move to the oxygen atoms; an especially favored Li⁺ complexation site appears in structure 2, where the regions of the negative potential of the two oxygen atoms overlap (Figure 4a).

In the direction perpendicular to the molecular plane a clear difference between boron and the aluminum acid center is visible. In the case of the TMB molecule there is a region of positive potential close to the boron atoms and methyl groups, with the effect of CH₃ groups prevailing. Moving further apart from the plane of the molecule one observes a rapid decay of this positive potential; at the distance of 4 Å it becomes completely screened out by the negative potential of oxygen atoms (Figure 4d). For TMAI the values of the positive potential close to the Al atom are much larger than those for the TMB; moreover, the basin of positive potential extends to larger distances and is still pronounced at about 5 Å from the molecular plane. This suggests that TMAI will be much more effective in the process of complexation of perchlorate ions.

In order to find the complex geometries we prepared a set of initial structures (about one hundred) with an ion placed close to the borane or aluminate molecule in a position chosen based on the analysis of the electrostatic potential. Then the geometry of the whole system was optimized in the B3LYP/6-31G** calculations. At this stage we observed that different initial structures lead to very similar complex geometries. This allowed us to select a set of representative structures which were then further optimized using a larger basis set aug-cc-pVDZ. The complexation energy was calculated as the difference between the energy of the whole system and the energies of complex components frozen at the complex geometry, corrected for a basis set superposition error (BSSE) using the counterpoise method.³⁵

Lithium Cations. The optimized structures of Li⁺ complexes with borane compounds resulting from the B3LYP/aug-cc-pVDZ calculations are shown in Figure 5. The geometries 1–4 are planar structures derived from the planar conformations of TMB or TMEB with Li⁺ located at about 1.8–1.9 Å from one or two oxygen atoms. The structure of the borane in the complex is only slightly distorted from the geometry of the isolated

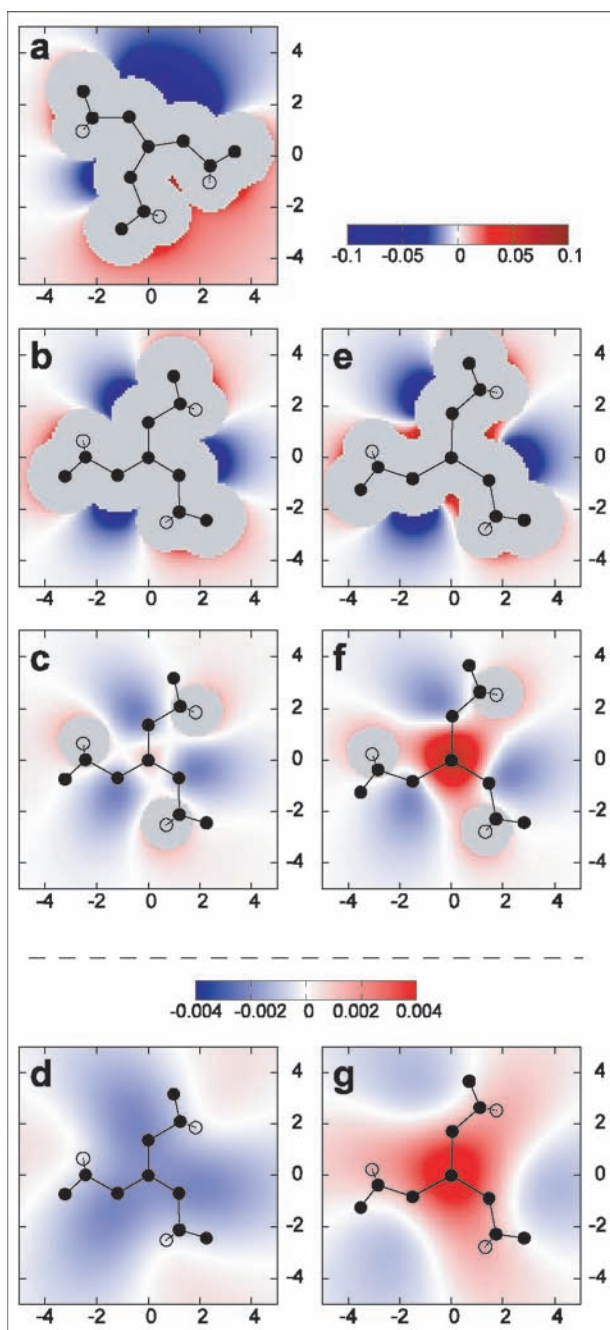


Figure 4. Electrostatic potential (in au) maps for selected TMB and TMAI conformers. Panel (a): potential in the plane of conformer 2 of TMB; panels (b)–(d) conformer 1-*t* of TMB, maps for planes at the distances of 0, 2, and 4 Å from the molecular plane, respectively; panels (e)–(g) plots for conformer 1-*t* of TMAI, plane selection as in plots (b)–(d). Points located closer than 1.5 Å to the nearest atom have been excluded from the plot (gray area). Note the different scale for the two bottom plots.

molecule. The complexation energy apparently correlates with the number of oxygen atoms to which the cation is coordinated. The energies presented in Figure 5 and other data not shown here lead to the conclusion that the energy of Li^+ complexation by one oxygen atom is in the range from -40 to -46 kcal/mol, while for the complexation by two oxygen atoms the stabilization increases by about 20 kcal/mol. The structures 5 and 6 are examples of nonplanar geometries allowing for larger coordination numbers and thus yielding larger complexation energies in the range of -80 to about -90 kcal/mol.

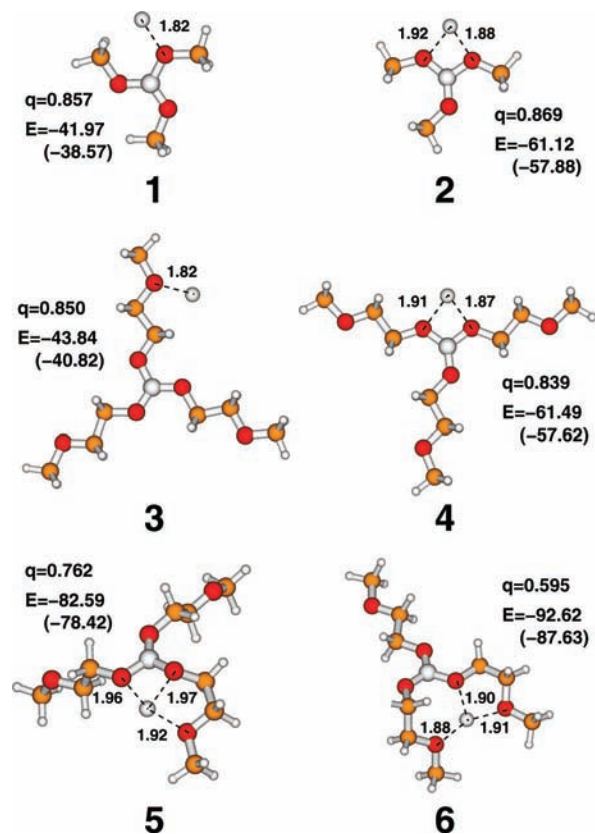


Figure 5. Structures of Li^+ complexes with TMB and TMEB calculated at the B3LYP/aug-cc-pVDZ level. Distances in Å; q is the partial charge on the ion resulting from the fit to the electrostatic potential; stabilization energies in kcal/mol, values in parentheses are single-point MP2 energies.

Figure 6 displays representative results obtained for lithium complexation by aluminum compounds. None of the geometry optimization runs produced an analogue of structure 1 from Figure 5; the sole structure of the Li^+ –TMAI complex is found (shown in Figure 6-1) independent of the initial geometry of TMAI. It has a larger stabilization (-68.9 kcal/mol) compared to its borane counterpart (-61.0 kcal/mol, Figure 5-2), which may be attributed to larger partial negative charges on oxygen atoms. It should be noted that in contrast to the borane complex, the geometry of TMAI distorts upon complexation. This is especially evident in the value of the Al–O–C angle, which increases from 130° in the isolated molecule to 155° in the complex.

Although some of the complexes of TMEAl with Li cations are planar (like structures 2 or 3; structure 4 is nonplanar in contrast to a similar configuration shown in Figure 5-4), in most of them the molecule is bent, and usually its geometry differs from that of the isolated molecule. Energies of TMEAl complexes with Li^+ coordinated to one or two oxygens are similar to those for borane complexes, being usually lower by 4–5 kcal/mol. On the other hand, there are structures such as 5 or 6, where the bending of the TMEAl molecule induces the shift of more oxygen atoms toward lithium cation, which makes it possible to achieve the coordination number of 4. Such complexes have significantly larger stabilization energy, as readily seen in Figure 6.

Generally, the stabilization energy of the Li^+ complex with the borane molecule increases with the number of coordinated oxygen atoms (about -40 , -60 , and -80 to -90 kcal/mol for one, two, or three oxygen atoms, respectively). The same dependence exists for aluminum compounds, in which case the

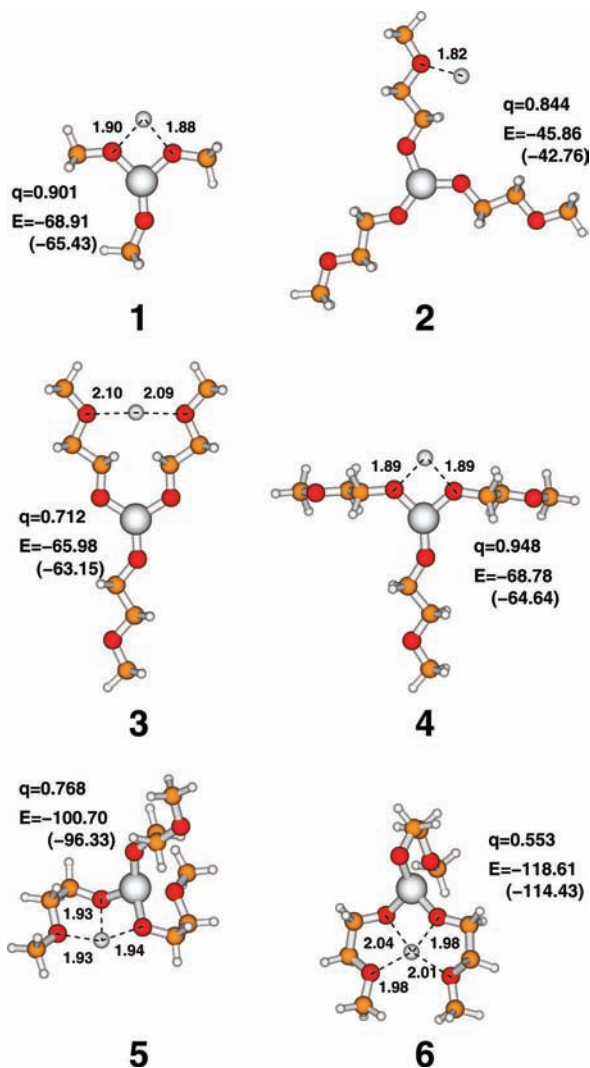


Figure 6. Structures of Li^+ complexes with TMAI and TMEAl calculated at the B3LYP/aug-cc-pVDZ level. The symbols are as in Figure 5.

complexes are more stable by 5–10 kcal/mol. Charge transfer between the molecule and the cation increases in the same order as readily seen from Figures 5 and 6; in the extreme case (Figure 6-6) the charge on lithium is only about $+0.5e$. The Li–O distance increases from about 1.8 Å to 2.05 Å with the coordination number increasing from 1 to 4. These findings are in good agreement with the energies and distances calculated in a study of Li^+ binding to polyalkyloxides,^{19,21} with the Li–O distance of 2 Å determined experimentally for LiClO_4^- complexes with diglyme³⁶ and with the maximum of the radial distribution function in the simulation of the PEO/ LiClO_4 electrolyte.^{37,38}

Complexation energies resulting from single-point MP2/aug-cc-pVDZ calculations in B3LYP/aug-cc-pVDZ geometries are shown in Figures 5 and 6 in parentheses. Apart from a minor decrease of the stabilization energy there are no significant differences with respect to the values obtained from DFT calculations.

We may conclude that the major effect of introducing B or Al atoms as Lewis acid centers into a PEO electrolyte on Li^+ complexation is the disruption in the sequence of polymer repeat units. This makes structures containing Li^+ coordinated to 6 oxygens less favored. On the other hand, the aluminum atom apparently provides some extra stabilization to the complexes with a lower coordination number.

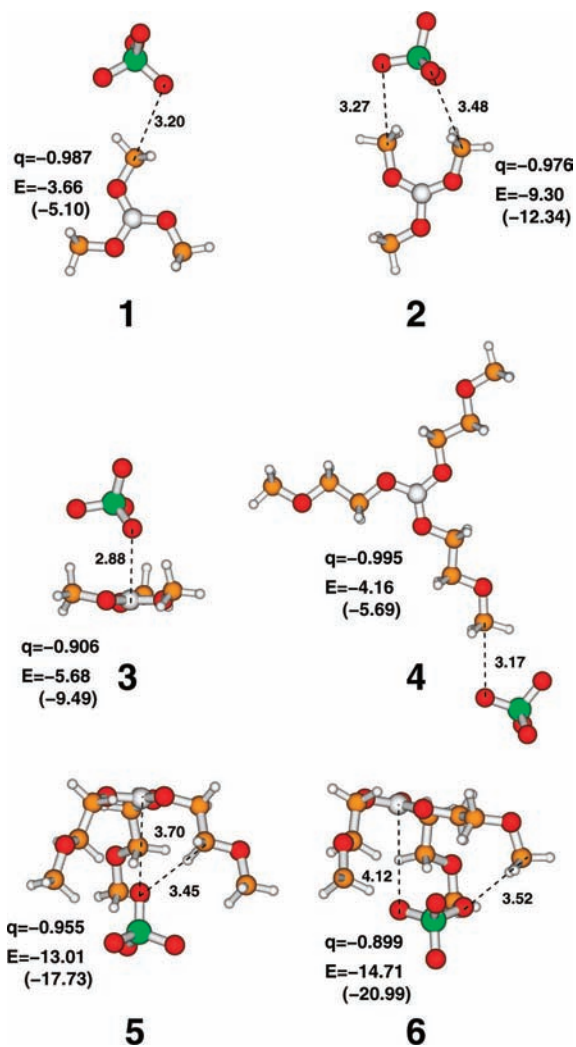


Figure 7. Structures of ClO_4^- complexes with TMB and TMEB calculated at the B3LYP/aug-cc-pVDZ level. Distances in Å; q is the partial charge on the perchlorate ion resulting from the fit to the electrostatic potential; stabilization energy of the complex in kcal/mol, values in parentheses are single-point MP2 energies.

Perchlorate Anions. As mentioned before, the conductivity increase in a Lewis acid-doped electrolyte is attributed to the trapping of ClO_4^- ions at acid centers. We will see in this section that the extent of such an effect differs by almost an order of magnitude between the borane and the aluminum compounds.

Selected final geometries of the perchlorate–borane complexes calculated at B3LYP/aug-cc-pVDZ are displayed in Figure 7. Optimization of the TMB– ClO_4^- complexes led to structures 1–3, depending on the initial conformation of the borane molecule and the initial position of the ion. In structures 1 and 2 the anion is located almost in the plane of the molecule in the region of positive electrostatic potential of methyl groups. In complex 2 the effects of two methyls accumulate which leads to significantly larger stabilization (–9.3 kcal/mol compared to –3.7 kcal/mol for structure 1). In structure 3 (of intermediate stabilization energy –5.7 kcal/mol) the perchlorate ion is located on top of the borane molecule at the B–Cl distance about 4 Å. As the electrostatic potential of the unperturbed TMB molecule is negative in this region, the formation of complex 3 cannot be explained merely by electrostatic interactions between permanent charges. However, it should be noted that the geometry of TMB changes in the complex, so that the CH_3 groups move toward the anion, which increases the attraction

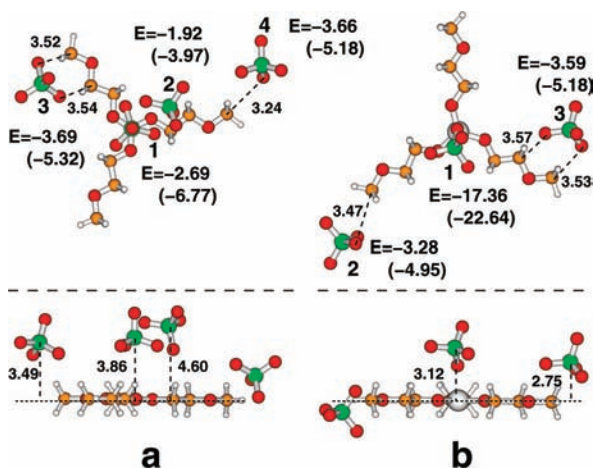


Figure 8. Structures of ClO_4^- complexes with the TMEB (a) or the TMEAl (b) molecule in frozen geometry. To save space all ion positions have been shown in a single figure. Upper panel: top view; bottom panel: side view. The symbols are as in Figure 7.

between the anion and the methyl groups compared to the complex with the borane molecule in planar conformation. Moreover, polarization of the molecule in the field of the ion leads to some additional stabilization.

Calculations for TMEB complexes led mainly to the structures in which the molecule is bent so that the alkoxy chains embrace the perchlorate ion (e.g., structures 5 and 6 in Figure 7), but several planar structures like geometry 4 can also be found. The planar structure 4 with perchlorate located close to the CH_3 group is equivalent to geometry 1 obtained for TMB. The complexation energies for both structures are therefore similar and close to -4 kcal/mol. Stabilization energies for bent structures may be as large as -13 to -15 kcal/mol, as seen for complexes 5 and 6. Depending on the initial geometry some structures with intermediate bending have been found (not shown in Figure 7), and their energies are in the range from -9 to -13 kcal/mol.

In most of the structures shown in Figure 7 the perchlorate anion is located near the CH_3 or CH_2 groups. This suggests that the primary effect stabilizing the perchlorate–borane complexes is the interaction of the anion with positively charged methylene or methyl groups from the polymer backbone. The interaction with the boron atom seems to be less important. In order to corroborate this conjecture we performed geometry optimization with the TMEB molecule frozen at the planar geometry of conformer 1 (Figure 2), allowing the perchlorate ion to find favorable sites of complexation. This made it possible to study the effects of ClO_4^- interaction with the B atom and with the CH_3 or CH_2 groups separately, unlike the calculations for a totally relaxed molecule, where the methyl groups move toward the ion. Freezing of the TMEB molecule may be more appropriate for studying the boron acid center in the polymer electrolyte; in this case the alkoxy groups are parts of the polymer backbone and have much fewer degrees of freedom than in the isolated borane molecule.

Repeating the calculations for different starting positions of the ClO_4^- ion we found several preferable locations of the perchlorate anion close to the borane molecule. For brevity we display them in a single figure (Figure 8a). In positions 1–3 the ion is located above the plane of the molecule; the distance from the Cl atom to the plane is between 3.5 and 4.6 Å. Position 1 corresponds to the tridentate orientation; flipping the ClO_4^- ion so that one of the Cl–O bonds points directly toward the boron atom results in a smaller stabilization energy of

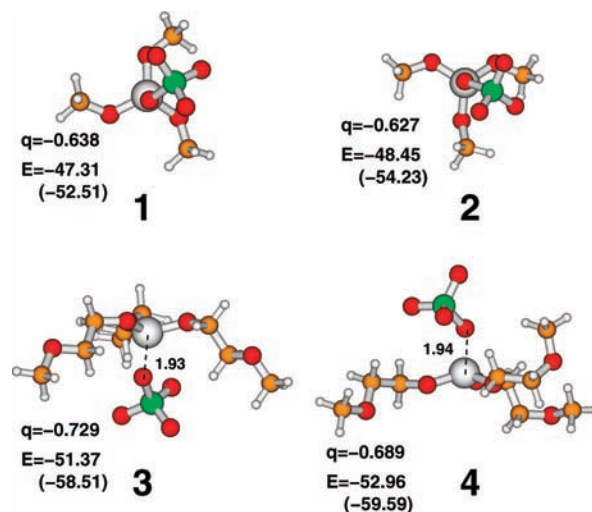


Figure 9. Structures of ClO_4^- complexes with TMAI and TMEAl calculated at the B3LYP/aug-cc-pVDZ level. The symbols are as in Figure 7.

-1.92 kcal/mol. In location 4 the perchlorate ion is only slightly above the plane of the TMEB molecule.

The results shown in Figure 8a lead us to the conclusion that the stabilization due to the interaction of the perchlorate anion with the boron center (between -1.9 and -2.7 kcal/mol depending on orientation) is weaker than that resulting from the interaction with the methyl group (-3.7 kcal/mol) and comparable to the interaction with the CH_2 units (-1.9 kcal/mol, location 2 in Figure 8a). Therefore, most of the stabilization in structures 5 and 6 in Figure 7 may be attributed to the interaction of the ClO_4^- ion with the positively charged CH_2 and CH_3 groups and not to the direct interaction with the boron atom. The above analysis allows us to interpret the results of previous calculations of the interaction energy for ClO_4^- –TMEB⁶ based on the hard and soft acids and bases theory. Comparing the values of the perchlorate ion interaction with pentaglyme and TMEB from Table 6 of ref 6 we can calculate the additional stabilization resulting from the presence of the boron center as -2.5 kcal/mol which agrees well with our stabilization energy of -2.7 kcal/mol obtained for configuration 1 in Figure 8a. Our present calculations give more information as to how the interaction energy depends on the complex geometry and how strong is the influence of methyl and methylene groups.

In Figure 9 we display selected structures of the ClO_4^- complexes with aluminum esters obtained in an unconstrained geometry optimization. In the case of the TMAI molecule no analogues of complexes 1 or 2 found for TMB (Figure 7) have been obtained; all calculations ended with the structure where the ion is located above the molecule slightly distorted from planar conformation; the distance from the Al atom to the nearest oxygen atom is 1.94 Å. Likewise, only nonplanar geometries have been found for the TMEAl complexes (structures 3 and 4 being representative examples). It is readily seen that the stabilization energy for all complexes is about -50 kcal/mol and is much higher than the stabilization for borane molecules. In all structures with TMEAl one of the perchlorate oxygen atoms approaches the aluminum atom quite closely (1.93–1.94 Å). This short distance and larger partial positive charge on the Al atom help us to understand the stabilization energies being almost four times larger than for boranes. Another effect of this close contact is the larger electron transfer: the partial charges on the ion derived from the electrostatic potential are

about -0.6 to -0.7 , compared to about -0.9 for borane complexes. This is another effect which may be responsible for weaker cation–anion interaction in the Lewis acid-doped electrolyte.

We have also performed geometry optimization for the perchlorate–TMEAl complex with constrained geometry of the aluminate molecule; results are shown in Figure 8b. As expected, the stabilization for the ion located in positions 2 or 3 close to the methyl group (about -3.5 kcal/mol) is similar to the corresponding value obtained for the borate complex. However, the interaction with the aluminum atom is much stronger (-17 kcal/mol compared to -2.5 kcal/mol). It is noticeable that the value of -17 kcal/mol for ion stabilization at the aluminum center in the complex is significantly smaller than the stabilization of fully relaxed complexes (about -50 kcal/mol). To examine this difference we performed additional calculations for the perchlorate ion interacting with the TMAI molecule frozen either in the geometry of an isolated molecule or in the geometry taken from structure 1 in Figure 9. In the former case the stabilization energy of the complex is about -13 kcal/mol; in the latter case the ion moves toward the position shown in Figure 9-1, with a corresponding gain in energy. We therefore conclude that changes in the geometry of the molecule around the Al atom (shift of the oxygen atoms away from the ion) are necessary to achieve large stabilization energies in the complex. A similar effect has been found in the case of TMB complexes but much less pronounced as the stabilization energies are smaller.

All geometry optimizations were done using the DFT method; we will briefly discuss additional single-point MP2/aug-cc-pVDZ calculations performed at geometries obtained from B3LYP optimizations (resulting complexation energies are shown in Figures 7–9). In all cases the stabilization energy of the complex calculated at the MP2 level is larger (up to 5–6 kcal/mol) than the value obtained within the DFT methodology; we attribute this effect to the dispersion interactions not accounted for adequately in DFT calculations. Closer inspection of the values obtained for frozen TMEB or TMAI molecules (Figure 9) reveals that the interaction with the CH_3 or CH_2 group increases by approximately 2 kcal/mol, and the stabilization of the anion at the boron or aluminum atom is about 5 kcal/mol larger. Although stabilization at the boron center is slightly larger than that at the methyl group, both effects are comparable, and the cumulated effect of perchlorate–methyl/methylene interactions will dominate the TMEB– ClO_4^- complexation.

From the results described in this section we may conclude that the interaction of the ClO_4^- ion with the Lewis acid center is much stronger for aluminate esters than for their boron equivalents; accordingly, aluminum centers will provide deeper traps for perchlorate ions.

IV. Conclusions

We have performed a search for preferred conformations of trimethoxyborane, tri(methoxyethoxy)borane, and their aluminum equivalents. The preferred geometry for TMB and TMAI is planar, with a 3-fold symmetry axis. The energy difference between cis and trans conformations of the terminal methyl groups in TMB is found not to exceed 1 kcal/mol. Structural parameters and the harmonic vibrational frequencies for the most stable conformer of TMB have been compared to the available experimental data. There is a difference between conformers of TMEB and TMEAl; planar and nonplanar conformers of the former molecule have comparable energy, while for the latter the bent conformations are much more stable (up to 25 kcal/

mol). The effect is attributed to a larger partial charge on the aluminum atom which allows larger electrostatic stabilization in the bent structures where oxygen atoms approach the aluminum center.

The main effect of the Lewis acid center on the Li^+ ion complexation by a polymer or plasticizer molecule appears to be a disruption of the sequence of PEO repeat units and introduction of an additional alkoxy chain at the boron or aluminum atom, which changes the local structure of the polymer and in this way affects the binding of the cation. Consequently, the polymer– Li^+ interaction energy in the vicinity of the acid center may be changed compared to an unmodified PEO. Nevertheless the stabilization energies obtained in this work are in the range found previously in the calculations for Li^+ –oligoglyme complexes.

A substantial quantitative difference between boranes and aluminate compounds has been found in perchlorate anion complexation. Interaction of the anion with the boron atom seems to be weaker than its interaction with the CH_2 and CH_3 groups carrying positive partial charges. The overall stabilization energy of the complex may be up to -15 kcal/mol, but only about 20–30% of this value may be attributed to the anion interaction with the boron atom. Interaction of ClO_4^- with an aluminum atom is much stronger. This leads to a different complex geometry and a large stabilization energy of about -40 to -50 kcal/mol. Therefore we may conclude that the effect of anion trapping at the aluminum centers in the electrolyte should be stronger than ion binding on boron sites, making the PEO with aluminum Lewis acids a prospective system for future experimental work.

The structural data gathered during our calculations may be used in the development of a force field suitable for a molecular dynamics study of boron and aluminum acid centers in PEO-based electrolytes, which will be the subject of future theoretical research.

Acknowledgment. The Gaussian03 calculations have been performed in the ACK “Cyfronet” computing center (grant no. MEiN/SGI3700/UJ/101/2006).

Supporting Information Available: Structural parameters for the lowest-energy conformer of trimethoxyborane. This material is available free of charge via the Internet at <http://pubs.acs.org>.

References and Notes

- (1) Mehta, M. A.; Fujinami, T. *Solid State Ionics* **1998**, *113–115*, 187.
- (2) Mehta, M. A.; Fujinami, T.; Inoue, S.; Matsushita, K.; Miwa, T.; Inoue, T. *Electrochim. Acta* **2000**, *45*, 1175.
- (3) Fujinami, T.; Mehta, M. A.; Sugie, K.; Mori, K. *Electrochim. Acta* **2000**, *45*, 1181.
- (4) Kato, Y.; Hasumi, K.; Yokoyama, S.; Yabe, T.; Ikuta, H.; Uchimoto, Y.; Wakihara, M. *Solid State Ionics* **2002**, *150*, 355.
- (5) Saito, M.; Ikuta, H.; Uchimoto, Y.; Wakihara, M.; Yokoyama, S.; Yabe, T.; Yamamoto, M. *J. Electrochem. Soc.* **2003**, *150*, A477.
- (6) Saito, M.; Ikuta, H.; Uchimoto, Y.; Wakihara, M.; Yokoyama, S.; Yabe, T.; Yamamoto, M. *J. Phys. Chem. B* **2003**, *107*, 11608.
- (7) Pennarun, P. Y.; Jannasch, P. *Solid State Ionics* **2005**, *176*, 1103.
- (8) Matsushita, K.; Shimazaki, Y.; Mehta, M. A.; Fujinami, T. *Solid State Ionics* **2000**, *133*, 295.
- (9) Fujinami, T.; Bozoujima, Y. *J. Power Sources* **2003**, *119–121*, 438.
- (10) Masuda, Y.; Seki, M.; Nakayama, M.; Wakihara, M.; Mita, H. *Solid State Ionics* **2006**, *177*, 843.
- (11) Jaffe, R. L.; Smith, G. D.; Yoon, D. Y. *J. Phys. Chem.* **1993**, *97*, 12745.
- (12) Muller-Plathe, F.; van Gunsteren, W. F. *Macromolecules* **1994**, *27*, 6040.
- (13) Gejji, S. P.; Tegenfeldt, J.; Lindgren, J. *Chem. Phys. Lett.* **1994**, *226*, 427.

- (14) Malysheva, L.; Klymenko, Y.; Onipko, A.; Valiokas, R.; Liedberg, B. *Chem. Phys. Lett.* **2003**, *370*, 451.
- (15) Klassen, B.; Aroca, R.; Nazri, G. A. *J. Phys. Chem.* **1996**, *100*, 9334.
- (16) Boinske, P. T.; Curtiss, L. A.; Halley, J. W.; Lin, B.; Sutjianto, A. *J. Comput.-Aided Mater. Des.* **1996**, *3*, 385.
- (17) Smith, G. D.; Jaffe, R. L.; Partridge, H. *J. Phys. Chem. A* **1997**, *101*, 1705.
- (18) Sutjianto, A.; Curtiss, L. A. *J. Phys. Chem. A* **1998**, *102*, 968.
- (19) Baboul, A. G.; Redfern, P. C.; Sutjianto, A.; Curtiss, L. A. *J. Am. Chem. Soc.* **1999**, *121*, 7220.
- (20) Gejji, S. P.; Gadre, S. R.; Barge, V. J. *Chem. Phys. Lett.* **2001**, *344*, 527.
- (21) Redfern, P. C.; Curtiss, L. A. *J. Power Sources* **2002**, *110*, 401.
- (22) Dhumal, N. R.; Gejji, S. P. *J. Phys. Chem. A* **2006**, *110*, 219.
- (23) Smith, G. D.; Jaffe, R. L.; Yoon, D. Y. *J. Phys. Chem.* **1993**, *97*, 12752.
- (24) Borodin, O.; Smith, G. D. *J. Phys. Chem. B* **2003**, *107*, 6801.
- (25) Borodin, O.; Douglas, R.; Smith, G. D.; Trouw, F.; Petrucci, S. J. *Phys. Chem. B* **2003**, *107*, 6813.
- (26) Borodin, O.; Smith, G. D.; Douglas, R. *J. Phys. Chem. B* **2003**, *107*, 6824.
- (27) Borodin, O.; Smith, G. D. *J. Phys. Chem. B* **2006**, *110*, 6279.
- (28) Borodin, O.; Smith, G. D. *J. Phys. Chem. B* **2006**, *110*, 6293.
- (29) Frisch, M. J.; Trucks, G. W.; Schlegel, H. B.; Scuseria, G. E.; Robb, M. A.; Cheeseman, J. R.; Montgomery, J. A., Jr.; Vreven, T.; Kudin, K. N.; Burant, J. C.; Millam, J. M.; Iyengar, S. S.; Tomasi, J.; Barone, V.; Mennucci, B.; Cossi, M.; Scalmani, G.; Rega, N.; Petersson, G. A.; Nakatsuji, H.; Hada, M.; Ehara, M.; Toyota, K.; Fukuda, R.; Hasegawa, J.; Ishida, M.; Nakajima, T.; Honda, Y.; Kitao, O.; Nakai, H.; Klene, M.; Li, X.; Knox, J. E.; Hratchian, H. P.; Cross, J. B.; Bakken, V.; Adamo, C.; Jaramillo, J.; Gomperts, R.; Stratmann, R. E.; Yazyev, O.; Austin, A. J.; Cammi, R.; Pomelli, C.; Ochterski, J. W.; Ayala, P. Y.; Morokuma, K.; Voth, G. A.; Salvador, P.; Dannenberg, J. J.; Zakrzewski, V. G.; Dapprich, S.; Daniels, A. D.; Strain, M. C.; Farkas, O.; Malick, D. K.; Rabuck, A. D.; Raghavachari, K.; Foresman, J. B.; Ortiz, J. V.; Cui, Q.; Baboul, A. G.; Clifford, S.; Cioslowski, J.; Stefanov, B. B.; Liu, G.; Liashenko, A.; Piskorz, P.; Komaromi, I.; Martin, R. L.; Fox, D. J.; Keith, T.; Al-Laham, M. A.; Peng, C. Y.; Nanayakkara, A.; Challacombe, M.; Gill, P. M. W.; Johnson, B.; Chen, W.; Wong, M. W.; Gonzalez, C.; Pople, J. A. *Gaussian 03*; Gaussian, Inc.: Wallingford, CT, 2004.
- (30) Manzanares, I. C.; Walla, D.; Seburg, R.; Wedlock, M. R.; Gonzalez, C.; Schlegel, H. B. *J. Chem. Phys.* **1991**, *95*, 3031.
- (31) Stampf, E. J.; Kim, Y. H.; Durig, J. R. *J. Raman Spectrosc.* **1993**, *24*, 725.
- (32) Gundersen, G. *J. Mol. Struct.* **1976**, *33*, 79.
- (33) Rogstad, A.; Cyvin, B. N.; Cyvin, S. J.; Brunvoll, J. *J. Mol. Struct.* **1976**, *35*, 121.
- (34) Besler, B. H.; Merz, K. M., Jr.; Kollman, P. A. *J. Comput. Chem.* **1990**, *11*, 431.
- (35) Boys, S. F.; Bernardi, F. *Mol. Phys.* **1970**, *19*, 553.
- (36) Henderson, W. A.; Brooks, N. R.; Brennessel, W. W.; Young, V. G., Jr. *J. Phys. Chem. A* **2004**, *108*, 225.
- (37) Halley, J. W.; Duan, Y.; Curtiss, L. A.; Baboul, A. G. *J. Chem. Phys.* **1999**, *111*, 3302.
- (38) Siqueira, L. J. A.; Ribeiro, M. C. C. *J. Chem. Phys.* **2005**, *122*, 194911.